Recent Glacier Changes in the Canadian Arctic

Martin Sharp[1,1], David O. Burgess[2], Fiona Cawkwell[3], Luke Copland[4], James A. Davis[1], Evelyn K. Dowdeswell[5,6], Julian A. Dowdeswell[6], Alex S. Gardner[1], Douglas Mair[7], Libo Wang[8], Scott N. Williamson[9], Gabriel J. Wolken[1], Faye Wyatt[1]

[1] Department of Earth and Atmospheric Sciences, University of Alberta; [2] Natural Resources Canada, National Glaciology Program; [3] Department of Geography, University College Cork; [4] Department of Geography, University of Ottawa; [5] Department of Geographical Sciences, University of Bristol; [6] Scott Polar Research Institute, University of Cambridge; [7] School of Geosciences – Geography and Environment, University of Aberdeen; [8.] Climate Research Division, Environment Canada; [9] Department of Biological Sciences, University of Alberta.

Abstract

The Canadian Arctic contains the largest area of land ice (~150,000 km^2) on Earth outside the ice sheets of Greenland and Antarctica and is a potentially significant contributor to global sea level change. The current ice cover includes large ice caps that are remnants of the Wisconsinan Laurentide and Innuitian ice sheets, and many smaller ice caps and valley glaciers that formed during the late Holocene. Most of these ice masses have decreased in area over the past century as a result of climate warming in the first half of the 20th century and since the mid 1980s. In general, smaller ice masses have lost a higher proportion of their area, but the largest total area losses have come from the larger ice caps. Both iceberg calving and negative surface mass balances have contributed to this episode of glacier shrinkage. Long-term calving rates are not well known, however, and many tidewater glaciers exhibit velocity variability on a range of timescales that may affect calving rates. Floating ice shelves in northern Ellesmere Island have lost over 90% of their area in the 20th century, with the most recent phase of disintegration occurring since 2000. Some fjords in the region are now ice free for the first time in over 3000 years.

[1] Corresponding author: Martin Sharp, Department of Earth and Atmospheric Sciences, University of Alberta, 1-26 Earth Science Building, University Campus NW, Edmonton, Alberta, T6G 2E3, Canada; martin.sharp@ualberta.ca

Introduction

The Canadian Arctic Islands (primarily Ellesmere, Axel Heiberg, Devon, Bylot and Baffin Islands) contain the largest ice covered area (over 150,000 km^2) on earth outside the ice sheets of Greenland and Antarctica. This amounts to 28% of the world's land ice area excluding the ice sheets. Mapping based on aerial photographs taken in 1959/60 gives glaciated areas of 107,488 km^2 in the Queen Elizabeth Islands (QEI), 37,652 km^2 in Baffin Island and 5,038 km^2 on Bylot Island. Since much of the Canadian Arctic is very thinly populated, the primary significance of its glaciers lies in their potential contribution to sea level change, the effects of which will be felt well beyond the region. More local impacts include the hazard to marine transport and offshore resource exploration and production that is posed by icebergs and ice islands calved from glaciers and ice shelves (which may become more significant as such activities increase as a result of a declining summer sea ice cover in the Arctic), and the effects of glacier retreat on water supply to some communities. Loss of the distinctive microbial ecosystems found on the surface of the ice shelves in northern Ellesmere Island, and in the epishelf lakes that they impound is also a concern as these ice shelves disintegrate (Vincent et al., 2009).

Scientific study of the region's glaciers dates back to the 1950's. Regional scale studies of the present-day ice cover have burgeoned in the past decade with the growing availability of remotely sensed datasets. These studies were stimulated to a large extent by the GLIMS project, which focuses on documenting changes in global glacier extent. However, they go beyond the scope of what was originally envisaged for GLIMS and include efforts to determine the mass balance of the regional ice cover, the role of climate forcing and ice dynamics in changes in mass balance and glacier extent, and the contribution of glaciers in Arctic Canada to global sea level change. Accordingly, this chapter describes the characteristics of the Canadian Arctic glacier cover, and the physiographic and climatic setting within which it has developed. It outlines recent trends in the regional climate and how these are reflected in the surface mass balance of glaciers, and describes efforts to use satellite remote sensing to develop ways to upscale glacier-specific surface mass balance measurements to the regional scale. It summarizes what is known of the dynamics of the larger ice caps in the region and the evidence that dynamics can (and do) change on relatively short time scales, and it describes what is known about the contribution of iceberg calving to the overall mass balance of the region. Finally, the chapter explains known about changes in the extent and volume of glaciers in the region since the end of the Little Ice Age and the contribution of glacier change to global sea level.

Regional Context

Geology and Physiography

The larger islands in the eastern Canadian Arctic (Ellesmere Island, Devon Island, Axel Heiberg Island, Bylot Island and Baffin Island) are rugged and mountainous. The highest peaks exceed 2000m in elevation and glacier ice covers much of the area (Figure 1), which was the source region of the Innuitian Ice Sheet during the last, Wisconsinan, glaciation (England et al., 2006). The northernmost parts of the Pre-Cambrian Canadian Shield are found in the east of this region on Baffin Island, eastern Devon Island and south-east Ellesmere Island. In southern Ellesmere and central Devon Islands, flat-lying rocks of Paleozoic age make up the Arctic Platform and form extensive, deeply dissected plateaus. To the north and west on Axel Heiberg, Devon and Ellesmere Islands, the Innuitian mountain system consists of sinuous belts of folded sedimentary rocks with a complex tectonic history.

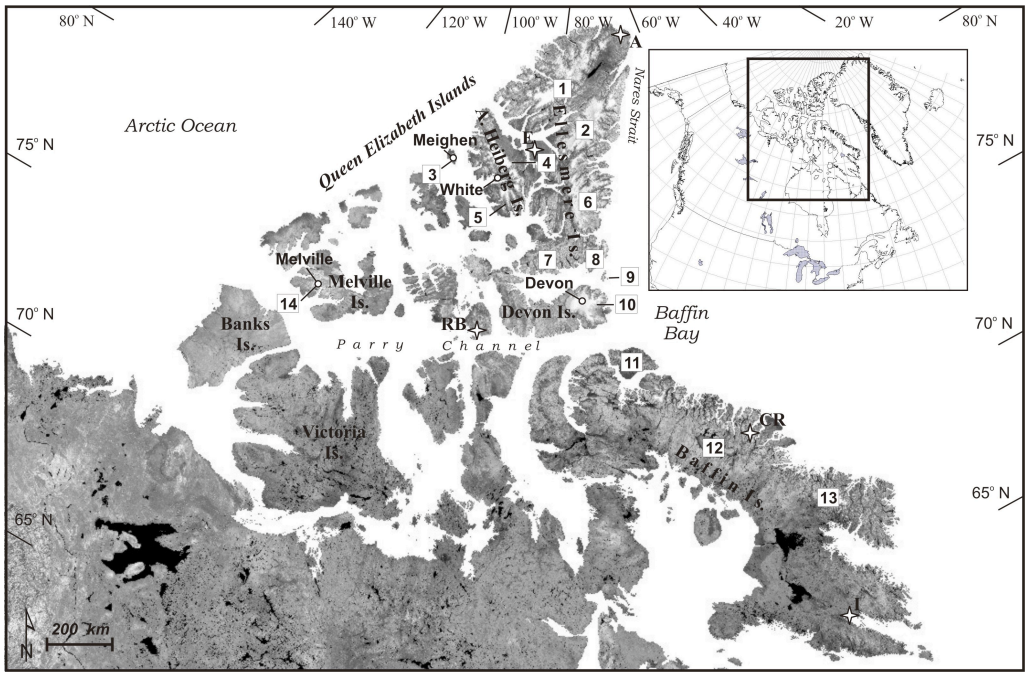

Figure 1: Radarsat 1 image mosaic of the Canadian Arctic showing the location of major ice caps and icefields (1: northern Ellesmere; 2:Aggasiz, 3: Meighen I.; 4: Mueller; 5: Steacie; 6: Prince of Wales; 7: Sydkap; 8: Manson; 9: Coburg I.; 10: Devon I.; 11: Bylot I.; 12: Barnes; 13: Penny; 14: Melville I.) , Environment Canada weather stations (A: Alert; E: Eureka; RB: Resolute Bay; CR: Clyde River; I: Iqaluit), and glaciers where surface mass balance is measured (in blue: Meighen I., White Glacier, Melville I., and Devon I.)

6/7/11 10:11 AM
Comment: Figure truncated and replaced as requested

Climate and Recent Climate Trends in the Canadian Arctic

There is a strong southeast to northwest precipitation gradient across the Canadian Arctic Archipelago, with an annual average precipitation of 420 mm in Iqaluit (southeast Baffin Island) and 70 mm in Eureka (central Ellesmere Island). Most of the region receives < 200 mm of precipitation per year. Records from Alert, Eureka, Resolute Bay, Clyde River, and Iqaluit (Figure 1) show strong seasonal cycles with over 70 % of annual precipitation falling in summer (JJA) and fall (SON) (Lesins et al., 2010). Although much of the summer precipitation falls as rain at the meteorological stations, which are located near sea level, most of it falls as snow at higher elevations over glaciers and ice caps. There is little inter-annual variability in total precipitation (20 – 100 mm a^{-1} for low and high precipitation sites respectively). Only records from Eureka and Resolute Bay show significant ($p < 0.05$) increases in mean annual precipitation (~7 mm per decade) over the period 1950-2007. However, precipitation is notoriously difficult to measure in Arctic areas and is likely underestimated in the station records.

Mean annual screen-level air temperatures vary with latitude, elevation, and distance from the ocean. They range from -20°C in central Ellesmere Island to -10°C in southern Baffin Island. Summer temperatures are of particular interest for understanding fluctuations in the mass balance of glaciers in the region. All stations registered an abrupt drop in mean July temperatures between 1961 and 1963 (Figure 2), and summer temperatures were generally lower (by ~ 0.75°C) from the mid 1960s to mid 1980s, than in the preceding and following periods. All stations except Clyde River display a significant positive trend in fall mean temperatures (SON; ~ +0.4 °C per decade) from 1950-2007.

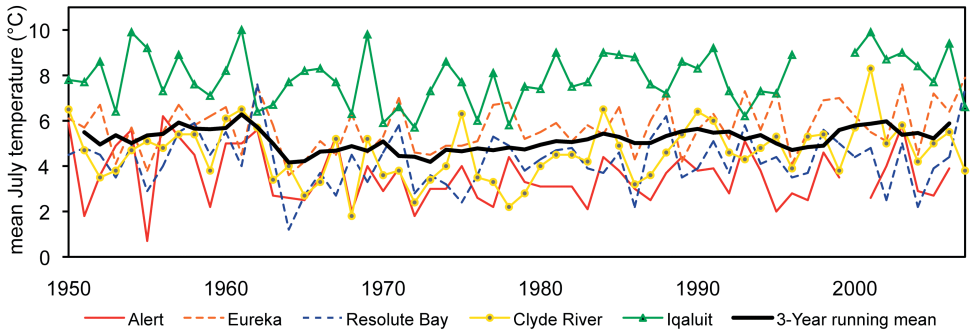

Figure 2: Mean July screen-level air temperatures for selected Environment Canada weather stations in the Canadian Arctic. Three year running mean is applied to all records (Source: http://www.climate.weatheroffice.ec.gc.ca).

Meteorological measurements in the Canadian Arctic are very sparse and biased towards coastal areas away from the mountainous regions where glaciers and ice caps are found. However, there is an

excellent correlation between summer air temperatures measured at the summit elevations of ice caps and large glaciers on Ellesmere and Devon Islands and 700 hPa air temperatures derived from climate reanalyses (Gardner and Sharp, 2009; Gardner et al., 2009). Reanalysis temperatures therefore provide a useful index of summer melt conditions across these glaciers. JJA 700 hPa decadal mean air temperatures were calculated for the period 1948-2008 from the NCEP/NCAR Reanalysis for regions centered over nine major glaciated sectors of the Canadian Arctic (Figure 3). They show strong positive anomalies in the 1950s and the 2000s, but negative anomalies in all other decades (particularly the 1960s (~ - 0.4°C) and 1970s (~ - 0.7°C). The warmest decade was the 1950s over Axel Heiberg and northern Ellesmere Islands (~ + 0.7°C), and the 2000s for Baffin Island, Devon Island and the rest of Ellesmere Island (+0.7 - +0.9°C). This history of summer air temperature change is similar to that of changes in the Atlantic Multidecadal Oscillation, a mode of variability in North Atlantic sea surface temperatures that involves alternating cold and warm phases that may last 20-40 years (Knight et al., 2006).

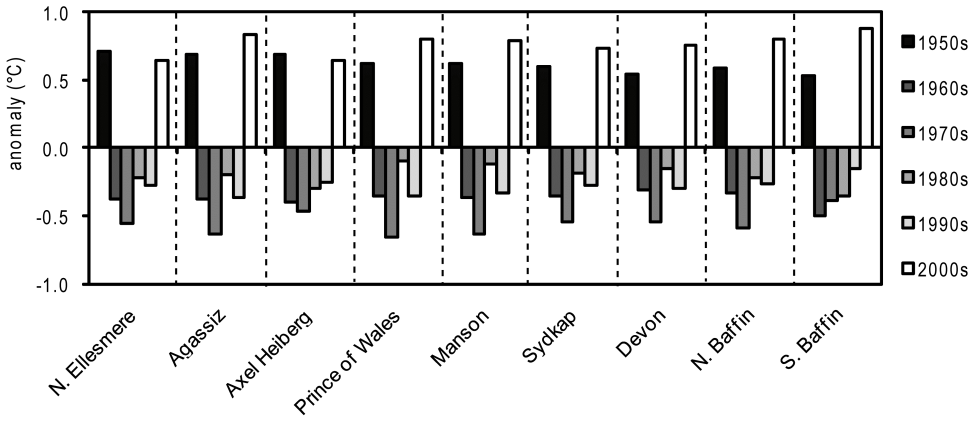

Figure 3: Decadal mean summer (JJA) temperature anomalies at 700 hPa over 9 major glaciated regions of the Canadian Arctic from the NCEP/NCAR Reanalysis for the period 1950-2008

North of 74°N, where much of the Canadian Arctic land ice is found, daily mean air temperatures over glaciers exceed the melting point temperature in only 2-3 months of the year. Peak temperatures occur in July (Figure 2), when most glacier melt occurs, and are a good proxy for glacier melt in the region. Inter-annual variations in mean July temperatures are controlled by the strength and

position of the July circumpolar vortex, a mid-tropospheric feature that consists of a cyclonic system with strong winds blowing counterclockwise about the cold polar air mass in its center (Gardner and Sharp, 2007). The vortex is the dominant factor in summer atmospheric circulation over the Arctic (Maxwell, 1980; Alt, 1987). When the vortex is strong (anomalously low mid-troposphere geopotential heights) and located in the western Hemisphere the mass of cold polar air is usually situated over the Canadian High Arctic and warm high pressure ridges that build over continental Canada are blocked from moving northward over this region, resulting in negative regional surface air temperature anomalies. When the vortex is weak (anomalously high mid-troposphere geopotential heights) and centered in the Eastern Hemisphere, warm continental high-pressure ridges can push northward and the Canadian High Arctic becomes thermally homogeneous with continental North America, resulting in positive regional surface air temperature anomalies. During the period 1963 to 2003, Gardner and Sharp (2007; their Figure 4) identified a significant shift from cooler to warmer mean July temperatures at Resolute Bay and Eureka after 1986-87 that was associated with increased occurrence of July vortex types that produced anomalously high surface air temperatures over the Canadian High Arctic.

More recent analysis reveals another significant shift in summer climate over the Queen Elizabeth Islands since 2005 (Sharp et al., 2011). Air temperature data from Environment Canada weather stations at Alert, Eureka, and Resolute Bay, from automatic weather stations on the Devon and Agassiz Ice Caps, from the NCEP/NCAR R1 Reanalysis (700 hPa level), and the MODIS11A2 land surface temperature (LST) dataset (MODIS subsetted land products, Collection 5; Oak Ridge National Laboratory Distributed Active Archive Center, 2010) are consistent in showing strong warming in the June-August period. T Eureka, for instance, 2009, 2005, 2007 and 2008 were four of the five warmest summers since records began in 1948. The mean summer temperature for 2005-2009 was warmer than that for 2000-2004 by 1.1°C on the Agassiz Ice Cap, and by 0.9°C on the Devon Ice Cap. Summer mean LSTs for 2005-2009 exceeded those for 2000-2004 by between 0.8°C (Devon Ice Cap) and 2.2°C (Axel Heiberg Island). The warmest summer in the LST record was 2005 in the southeast of the Queen Elizabeth Islands (Devon Ice Cap) and either 2007 or 2008 in the north and west (Sharp et al., 2011). This recent period of anomalously warm summer temperatures has been associated with an atmospheric circulation configuration that favors strong heat advection from the northwest Atlantic (where sea surface temperatures have been unusually warm) into the Queen Elizabeth Islands (Sharp et al., 2011; Sharp and Wolken, 2011).

Glacier Characteristics

Over 70% of the glaciated area of the Canadian Arctic Islands is accounted for by eleven large ice caps and icefields (Figure 1), while the rest consists of smaller plateau ice caps and valley glaciers distributed across the region. The glacier cover is concentrated in the mountains facing Baffin Bay in the east and the Arctic Ocean in the north and west. The Barnes Ice Cap is situated on a plateau in the interior of Baffin Island and is probably a remnant of the late Wisconsinan Laurentide ice sheet. All the major ice caps/icefields in the QEI are drained in part by tidewater terminating outlet glaciers (of which there are 279 in the QEI), though significant sections of their margins do terminate on land. The proportion of ice cap area that drains to tidewater ranges from 6% (Sydkap, Ellesmere Island) to 66% (Prince of Wales Icefield, Ellesmere Island). There is widespread evidence of glacier surging (Copland et al., 2003), and significant seasonal velocity variations have been observed on many glaciers in the region (Cress and Wyness, 1961; Iken, 1974; Bingham et al., 2003, 2008; Williamson et al., 2008). Some of these variations are clearly driven by seasonal penetration of surface meltwater to the glacier bed (Iken, 1974; Boon and Sharp, 2003; Bingham et al., 2006). The only floating ice shelves in the northern hemisphere, composed of a mixture of saline and freshwater ice, fringe the northern coast of Ellesmere Island (Jeffries, 1992).

Stable isotope records from ice cores (Paterson et al., 1977; Hooke and Clausen, 1982; Fisher et al., 1983, 1995, 1998; Zdanowicz et al., 2002; Kinnard et al., 2008) show that a number of the larger ice caps in Arctic Canada contain isotopically distinct ice dating from the last glaciation. Although these ice caps have survived throughout the Holocene, there is good evidence that many of the region's smaller ice caps and glaciers disappeared in the early- to mid-Holocene and subsequently re-formed (Koerner and Fisher, 2002). The large-scale pattern of deglaciation of the late Wisconsinan Innuitian Ice Sheet (that covered most, if not all, of the QEI) after 11 ^{14}C ka BP is now relatively well known (England et al., 2006). In the Baffin Bay and Nares Strait regions, the ice margin reached the current eastern limits of the Devon Island Ice Cap and Manson and Prince of Wales Icefields between 10 and 8 ^{14}C ka BP, and of the Agassiz Ice Cap after 7.5 ^{14}C ka BP. In most places, it reached the current western limits of these ice caps after 8 ^{14}C ka BP. On northern Ellesmere and Axel Heiberg Islands, deglaciation to current margins occurred after 8.5 ^{14}C ka BP, and probably later on the eastern than on the western sides of these ice caps.

Small ice caps have been present in the interior of northern Baffin Island for 1600 to 2800 years, but the plateau on which they occur appears to have been ice free throughout the middle Holocene

(Anderson et al., 2008). Ice cap growth in that region became widespread around 1280 AD and intensified around 1450 AD. There is evidence from several sites on Ellesmere and Axel Heiberg Islands for glacier advances post-dating 1000 ^{14}C ka BP that resulted in maximum glacier extents in the late 19th or early 20th centuries (Blake, 1981).

Special Topics: Regional Glacier Mass Balance and Proxy Indicators

Surface Mass Balance and Mass Balance Changes

The highest density of long-term (>40 yrs) records of glacier surface mass balance in the Arctic is from the Canadian Arctic Archipelago. These records provide an important context for understanding observed glacier changes and their relationship to climate trends, but they are all from glaciers located north of 74 °N. There are no long-term measurements from Bylot or Baffin Islands, so little is known about the current mass balance of glaciers in the southern part of the region. Koerner (2002, 2005) and Andrews et al. (2002) respectively summarize past mass balance measurements in the QEI and on Baffin Island, while Cogley and others (1996) provide a discussion of the associated errors.

In the Canadian High Arctic (> 74°N), inter-annual variability in the summer (JJA) mass balance far exceeds that in the winter balance. As variability in the summer balance accounts for more than 90% of the variance in the annual balance (Koerner, 2005) (Figure 4), this can be explained largely in terms of summer melt, which occurs primarily in July.

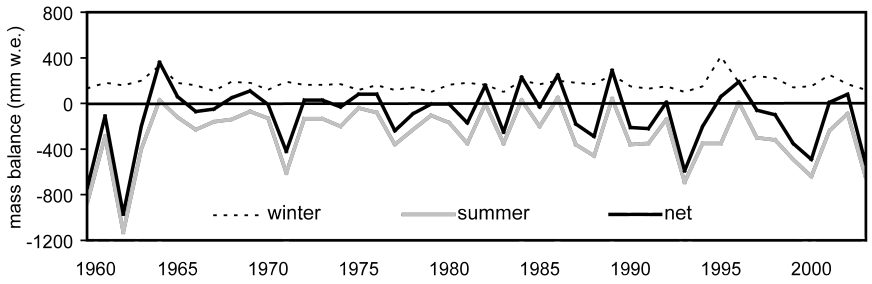

Figure 4: Winter, summer and annual net surface mass balance of the Meighen Island Ice Cap (R.M.Koerner, personal communication).

For the period 1963-2003, Gardner and Sharp (2007) used Principal Components Analysis to extract a regional signal from the long-term surface mass balance records from the Devon Island Ice

Cap, Meighen Ice Cap, Melville Island South Ice Cap (Koerner, 2005), and White Glacier (Axel Heiberg Island; Cogley et al., 1996) (Figure 5). The regional glacier surface mass balance became increasingly negative after 1987, as the incidence of westerly positions of the July circumpolar vortex decreased and July mean air temperatures at Eureka and Resolute Bay increased (Lesins et al., 2010). This trend has been accentuated since 1998. 9 of the 11 most negative balance years in the 48 year record from the Devon Island Ice Cap have occurred in that period, coincident with strongly positive 700 hPa summer temperature anomalies in the NCEP/NCAR Reanalysis. Cumulative mass balances over the periods of measurement are – 5.20 m w.e. for Devon Island Ice Cap (1961-2009) and - 7.62 m w.e. for White Glacier (1960-2008, with three missing years, 1980-82). Over 75% of the measured surface mass loss from both glaciers occurred after 1987 (46% of the measurement period), and over 60% of that from the Devon Island Ice Cap since 1998. Between 30 and 48% of the measured mass loss from the 4 measured glaciers since 1963 has occurred since 2005, in response to the recent summer warming. The mean mass loss rate from these 4 glaciers in the 2005-2009 period (-493 kg m^{-2} a^{-1}) was nearly five times the mean for 1963-2009, and it was seven times greater in 2007 and 2008 (-698 kg m^{-2} a^{-1}) (Sharp et al., 2011).

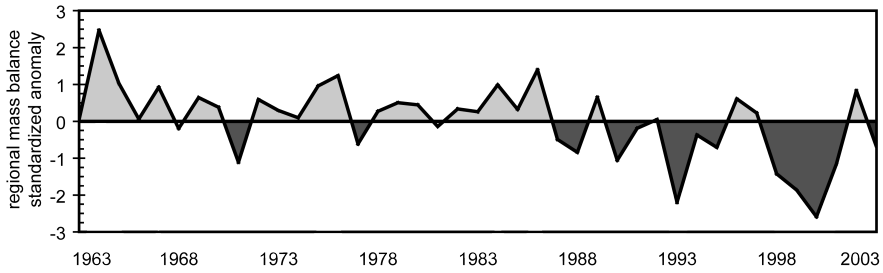

Figure 5: Standardized anomalies of the Canadian High Arctic regional glacier surface mass balance (after Gardner and Sharp, 2007).

The occurrence of July vortex types associated with warm temperatures and negative mass balance anomalies was also high in the period 1948-62, consistent with high screen level temperatures (Figure 2) and positive decadal anomalies in 700 hPa air temperatures over the Canadian Arctic islands in the NCEP/NCAR Reanalysis (Figure 3). Thus, the 1950's was probably also a decade of strongly negative surface mass balances in the region.

Summer Melt

Given the limited number of surface mass balance records for the Canadian Arctic, efforts have been made to develop remote sensing methods for upscaling the records available to the regional ice cover. These methods focus on regional scale mapping of parameters that are expected to be well correlated with glacier surface mass balance, and exploit the availability of enhanced resolution (2.225 or 4.5 km) data products from the Ku-band SeaWinds scatterometer on NASA's QuikScat satellite (Wang et al., 2005; Wolken et al., 2009). These products provide twice daily measurements of the normalized radar cross-section (backscatter coefficient, σ^0) over high latitude regions from summer 1999 to summer 2009. This parameter is very sensitive to the presence of water on glacier surfaces and can therefore be used to map the duration of summer melt across the whole region. If there is a correlation between the duration and magnitude of summer melt, the maps produced should provide useful information about regional variations in surface mass balance because it is so sensitive to inter-annual variations in the amount of summer melting.

Wang et al. (2005) mapped summer melt duration over the QEI ice caps for the period 2000-2004 (Figure 6). Comparison with surface air temperature measurements from the Prince of Wales Icefield, Ellesmere Island, for 2001 revealed a strong positive relationship between melt duration and seasonal positive degree day totals (a parameter used to drive temperature index surface mass balance models). The 5-year mean melt duration (Figure 6) varies systematically with elevation and distance from the Baffin Bay heat and moisture source. The mean length of the melt season ranges from 1 day at the highest elevations on the Agassiz Ice Cap (Ellesmere Island) to 100 days at low elevations on ice caps facing Baffin Bay. Low elevation margins facing the Arctic Ocean have longer melt seasons than margins facing the interior of the QEI, which are generally at higher elevations. The mean melt duration for the QEI ice caps is 37.7 +/- 4.9 days. Within the 5-year period, 2001 (42.6 days) and 2003 (41.4 days) stand out as the longest melt seasons (averaged over all ice caps), and 2002 (30.9 days) as the shortest. This is consistent with NCEP/NCAR Reanalysis JJA 700 hPa temperatures for the region. Interestingly, the signs of melt duration anomalies in a given year can be opposite at high and low elevations on a given ice cap (most notably on the Prince of Wales Icefield and Devon Island Ice Cap). Recently, the QuikScat-derived melt duration record has been extended to 2009, revealing that 2005, 2007 and 2008 had unusually long melt seasons, and 2006 and 2009 has shorter than average melt seasons in most regions of the Queen Elizabeth Islands (Sharp et al., 2011). This is fully consistent with the evidence for warmer summers in the region since 2005 presented above.

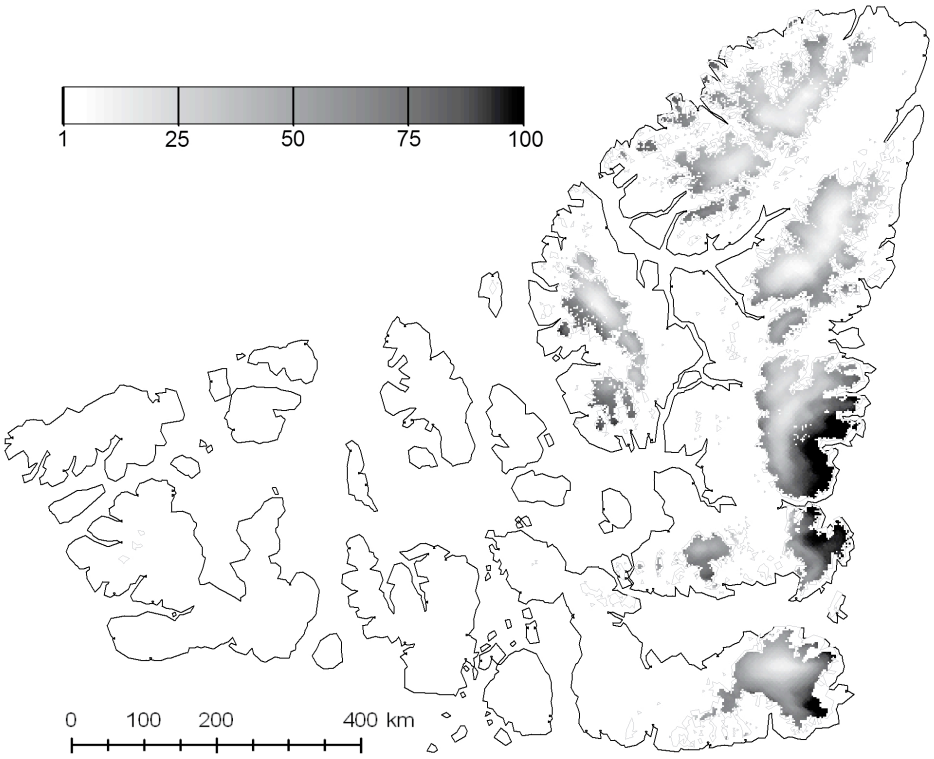

Figure 6: Annual mean melt duration (days) over glaciers in the Queen Elizabeth Islands for the period 2000-2004 derived from enhanced resolution QuikScat backscatter coefficient products.

When averaged over a two-week period beginning two weeks after the end of the melt season, QuikScat σ^0 data display systematic patterns of variability across the Canadian Arctic ice caps. Typically, σ^0 is high over high elevation interior regions and decreases in a stepped manner towards the ice cap margins (Wolken et al., 2009). Comparison of the σ^0 pattern on the south side of the Devon Island Ice Cap in September 2004 with concurrent snow and firn stratigraphy (Bell et al., 2008) showed that the σ^0 pattern broadly reflects the distribution of the percolation, saturation, superimposed ice, and glacier ice facies (Benson, 1962) at the end of the melt season. ISODATA classification methods

applied to the σ^0 data allow the facies to be mapped on a regional scale (Figure 7). For the period 1999-2005, glacier ice was the most extensive facies on QEI ice caps (26.7% of the total ice covered area), followed by the saturation, percolation, and superimposed ice zones (26.0%, 23.7%, and 23.6% respectively). However, the relative proportions of the different facies vary significantly between ice caps. The superimposed ice facies is especially important on low elevation ice caps in the south east that experience high accumulation (Manson, Sydkap), while the percolation facies is more widespread in the colder, drier regions of the north (Agassiz and northern Ellesmere).

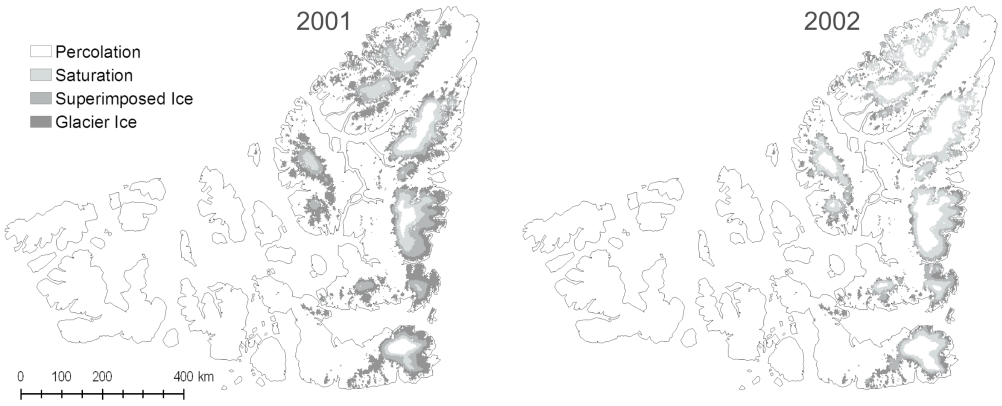

Figure 7: Comparison of end of summer snow/ice facies distributions on glaciers in the Queen Elizabeth Islands for 2001 (long melt season – mean of 43 d) and 2002 (short melt season – mean of 31 d).

Facies distributions vary significantly between years (Figure 7). Changes in the areas of the superimposed and glacier ice zones correlate negatively with percolation and saturation zone area changes. 2001 stands out as a year with unusually extensive areas of glacier and superimposed ice at the end of the melt season on all major ice caps, while the area of these facies was unusually low in 2002 and 2004. This is consistent with surface mass balance data, which indicate that 2001 was a very negative balance year (the most negative between 1961 and 2005 on the Devon Island Ice Cap) while surface balance in 2002 and 2004 was only slightly negative, or even positive, at all sites for which data are available. Changes in summer mid-troposphere geopotential height and air temperature correlate positively with changes in the area of the glacier ice facies, negatively with the area of the percolation

and saturation facies, and positively with changes in inter-facies boundary elevations. Regular end of summer mapping of facies areas and inter-facies boundary elevations therefore offers another way to investigate regional scale climate and mass balance conditions across Arctic ice caps. Note that the end of summer position of the boundary between the glacier ice and superimposed ice facies denotes the annual equilibrium line altitude and can be used to define the accumulation area ratio of a glacier or ice cap.

Ice Flow and Iceberg Calving Fluxes

Many of the large ice caps in the Canadian Arctic are drained in part by large tidewater outlet glaciers that lose mass by calving icebergs into the ocean. Any assessment of regional mass balance must therefore take account of the contribution of calving to overall mass loss. For this to be possible, it is necessary to know the rate of glacier flow and the cross sectional area of each outlet glacier at its terminus, and the history of terminus fluctuations over the time period for which the calculation is to be made.

Burgess et al. (2005) carried out the first synoptic scale mapping of the surface velocity field of the Devon Island Ice Cap using synthetic aperture radar interferometry (InSAR) and speckle tracking methods applied to data from the ERS 1/2 (tandem mode mission) and RadarSat satellites. Measurements were derived from data acquired during the winter, so they will underestimate the annual mean velocity if the surface velocity increases in summer (e.g. Williamson et al., 2008). The ice cap has a dynamic structure similar to that of the large ice sheets in Greenland and Antarctica. Most of the ice cap flows at very low velocities, but a large fraction of its volume drains to the ocean via 18 fast-flowing outlet glaciers. Peak velocities in the largest of these glaciers exceed 100 m a^{-1} and reach nearly 300 m a^{-1}. The iceberg calving flux from the ice cap (-0.52 +/- 0.14 Gt a^{-1}; calving fluxes are assigned a negative sign as they contribute to mass loss from an ice mass) was estimated by combining the measured surface velocities with ice thickness measurements derived from airborne radio echo sounding (Dowdeswell et al., 2004) and measurements of changes in the terminus position of major outlet glaciers between 1960 and 1999 (Burgess et al., 2005). This represents about 30% of the total mass loss from the Devon Island Ice Cap over the period 1960-99, and about half of it comes from a single source – the Belcher Glacier in the north-east of the ice cap.

Williamson et al. (2008) used image intensity domain cross-correlation methods (Scambos et al., 1992) and LandSat7 ETM+ images to measure the surface velocity of tidewater outlet glaciers draining

the Agassiz Ice Cap, and combined them with Dowdeswell's centreline ice thickness measurements to estimate iceberg calving fluxes. There were large (up to an order of magnitude) seasonal variations in both surface velocity and calving rates. Annual mean velocities of the largest outlets were up to 400-700 m a^{-1}. Summer calving rates were 2-8 times higher than annual mean rates and terminus retreat was a large contributor to summer calving fluxes (1.7 times the contribution from ice flux through the terminus on average). The estimated mean annual calving flux from the ice cap (- 0.61 +/- 0.14 Gt a^{-1}) was comparable to that from the Devon Island Ice Cap, and a single glacier (Eugenie Glacier) accounted for 54% of the total flux. Iceberg calving fluxes were also calculated for Otto Glacier in northern Ellesmere Island by Williamson et al. (2008) and by Short and Gray (2005; using radar speckle tracking methods applied to Radarsat data to determine glacier velocities). Both flow velocities and calving fluxes from this glacier exhibit large temporal variability, and calving flux estimates ranged from - 0.11 to - 0.56 Gt a^{-1}.

Calving fluxes for major outlet glaciers draining the Prince of Wales Icefield were estimated using surface velocities derived from RadarSat data by speckle tracking (Short and Gray, 2005) and cross-glacier measurements of ice thickness made with the University of Kansas ice penetrating radar system in 2005 (Mair et al., 2009). Surface velocities ranged from 350 (Ekblaw Glacier) to 650 (Trinity Glacier) m a^{-1} (Short and Gray, 2005). The calving flux due to flux at the glacier margins was estimated to be -1.65 ± 0.21 Gt. a^{-1}, and that due to terminus retreat to be -0.27 ± 0.03 Gt. a^{-1} for a total mass loss due to calving of -1.92 ± 0.21 Gt. a^{-1}. The bulk of this flux (over 80%) comes from a single source – the combined terminus of the Trinity and Wykeham Glaciers.

The total calving flux from calving sources so far investigated in the QEI is -3.4 +/- 0.28 Gt a^{-1}. Fluxes have yet to be determined for Sydkap, Manson Icefield, Axel Heiberg Island and much of northern Ellesmere Island. Short-term variability in both the velocity and terminus position of the major calving glaciers may not be well captured by the existing analyses, and represents a source of uncertainty in the calving flux estimates. Nonetheless, calving is clearly a significant loss term in the mass budgets of these ice caps. One or two glaciers may dominate the calving flux from an entire ice cap.

Case Studies

Surge-Type Glaciers

Although there are few direct observations of glacier surges in the Canadian Arctic (Hattersley-Smith, 1964, 1969; Mueller, 1969; Copland et al., 2003), 1:60,000 aerial photographs from ca 1960 and

Landsat 7 ETM+ satellite imagery from ca. 2000 suggest that surge-type behavior may be quite widespread in the region (Copland et al., 2003; Dowdeswell et al., 2007). Various features provide evidence of past surge activity, including looped or deformed moraines, anomalous and/or widespread crevassing, stagnant ice, potholes on the glacier surface, and over-steepened termini (Meier and Post, 1969; Sturm, 1987). In the QEI, Copland et al. (2003) identified 51 glaciers that showed evidence of past surge activity, 15 of which were apparently actively surging in either 1959/60 or 1999/2000. On Bylot Island, distorted medial moraines and over-steepened margins are the most commonly observed surge indicators (Dowdeswell et al., 2007). Most of the 10 glaciers with ice-surface features indicative of possible surge activity are situated along the northeast coastline of Bylot Island, and none are located along the northwestern portion of the island or the southern margin. There is some evidence of past surging along the southern margin of the Barnes Ice Cap (Løken, 1969; Holdsworth, 1973, 1977), but there has been no systematic survey to identify surge type glaciers on Baffin Island.

In the QEI, most surge type glaciers appear to be large tidewater outlet glaciers that drain regions of relatively high snowfall. The highest concentration of surge type glaciers is found on the north and east sides of the Manson Icefield, Ellesmere Island. The active phase of surging appears to last many years, and it is likely that the quiescent phase is also very long, although repeat surging has rarely been observed. Some surges have resulted in large advances of glacier termini. For instance, On Axel Heiberg Island, Good Friday, Iceberg, and Airdrop Glaciers all advanced between 4 and 7 km between 1959 and 1999 (Copland et al., 2003). Since 2000, two surges have begun on the Agassiz Ice Cap: Parrish (peak velocities 2006-7) and Dobbin (peak velocities 2005-6) Glaciers.

The biggest surge so far observed is that of Mittie Glacier, which drains northwards from the Manson Icefield (Plate 1). This glacier was surging in 1999 (Copland et al., 2003) and continued to surge until 2008 by which time its terminus had advanced over 4 km relative to its position on 1959 aerial photographs. Velocities of Mittie Glacier during its surge (which peaked at > 1.3 km/yr in 1999-2000 or earlier) were determined from Landsat 7 ETM+ imagery using image cross-correlation methods (both intensity domain cross-correlation (Scambos et al., 2002; Dowdeswell and Benham, 2003; Copland et al., 2003) and an automated variable correlation block size algorithm implemented in the frequency domain based on intensity gradient correlation (Fitch et al., 2002)). The latter method involves cross correlation of co-registered intensity gradient images (Plate 2). Haug et al (2010) also used the intensity gradient method to derive ice flow velocities, but with a fixed correlation block size. The method is useful for determining velocities from images that contain data gaps, such as post-2003

Landsat 7 images, which are affected by "striping" (Plate 2). However, the fixed correlation block size approach does not work well on actively surging glaciers because of the large spatial gradients in velocities that can occur between surging and stagnant regions of the glacier, and between the surging glacier and non-surging tributaries. Plate 2 illustrates how the automated variable correlation block size resolution algorithm can detect large spatial gradients in velocity in a single run of the algorithm. With the fixed correlation block size approach, it would have been necessary to run the cross correlation many times at different correlation block sizes to achieve this result.

Northern Ellesmere Island Ice Shelves

Floating ice shelves are found along the northern coast of Ellesmere Island. Jeffries, (1992) identified three main types of ice shelf on the basis of their composition – sea ice (e.g. Ward Hunt Ice Shelf), glacier ice (Milne Ice Shelf), or a mixture of the two (Alfred Ernest Ice Shelf, recently renamed the Serson Ice Shelf). Radiocarbon dating of driftwood accumulations on shorelines behind the present-day sea-ice ice shelves indicates that driftwood deposition ceased and formation of these ice shelves began around 5500 ^{14}C years BP (England et al., 2008). In the early 20th century, a single ice shelf with an area of 7500 km^2 extended along the length of the northern Ellesmere Island coastline (Jeffries 1987). Over the past century this feature has fragmented into a diminishing number of smaller ice shelves, with a total area of 943 km^2 by the end of summer 2005 (Copland et al., 2007) and 720 km^2 by the end of summer 2008 (Mueller et al., 2008). This fragmentation has resulted in the release of a number of very large icebergs or "ice islands" into the Arctic Ocean. The biggest of these, T-2, had an area of 700 km^2 (Koenig et al., 1952). Disintegration occurred in two main phases – before the 1950's (Koenig et al., 1952) and after 2000 (Mueller et al., 2003; Copland et al., 2007; Mueller et al., 2008), with some significant calving events in the early 1960's (Hattersley-Smith, 1963). The most recent phase of disintegration has resulted in large reductions in the remaining ice shelf area. Between 2000 and 2002, the Ward Hunt Ice Shelf broke in two (Mueller et al., 2003). In August 2005, the Ayles Ice Shelf broke up (Copland et al., 2007) and, in 2008, the area of the remaining ice shelves in the QEI decreased by 23% with a 60% area loss of Serson Ice Shelf and the complete disintegration of the Markham Ice Shelf (Mueller et al., 2008). Conditions favoring ice shelf disintegration seem to include long-term thinning and weakening due to warming climate and negative surface mass balance (Braun et al., 2004; Copland et al., 2007), persistent offshore winds (Ahlnäs and Sackinger, 1988; Copland et al., 2007), and the loss of buttressing from thick multi-year sea ice (Copland et al., 2007, Mueller et al., 2008).

Monitoring of recent ice shelf breakup events on northern Ellesmere Island has benefited greatly from the development of new satellite sensors that can see further north than earlier sensors. For example, ASTER is able to view regions up to ~84°N with the use of pointing, whereas Landsat sensors were typically unable to image ice shelves due to their inability to image areas further north than ~80°N. In addition, the frequent repeat imaging of high latitude regions by the MODIS sensor (on both the TERRA and AQUA satellites) has enabled the near real-time monitoring of ice shelf breakup events (Plate 3). This is in large part due to the convergence of satellite orbits near the poles that enables imaging at intervals of one hour or less. These developments mean that much more is known about the ice shelf breakup events that have occurred in the first decade of the 21st century than about many of the ice shelf breakup events that occurred in the 20th century (Copland et al., 2007; Mueller et al., 2008). For example, Plate 3 shows how almost the entire Ayles ice shelf calved away from northern Ellesmere Island within a few hours in August 2005.

Regional Synthesis: Recent Changes in Equilibrium Line Altitude and Glacier Extent

Methodology

Satellite Imagery (Plate 4), and aerial photography flown between 1956 and 1961 have been used to delineate the extent of glaciers in Arctic Canada in the late nineteenth/early twentieth century (defined by end moraines and trimlines), and around 1960, 1975, 1993 and 2000 (Sharp et al., 2003; Dowdeswell et al., 2007; Wolken, 2006; Wolken et al., 2008a; Svoboda and Paul, 2009).

Late 19th century ice extents were determined using a combination of automated/semi-automated image classification to map recently deglaciated terrain (Wolken, 2006; Wolken et al., 2008a; Plate 4), and manual digitization of end moraines and/or trimlines visible on aerial photographs and/or satellite imagery (Svoboda and Paul, 2009). For mapping recently deglaciated terrain in the QEI, automated classification methods using the ratio ETM+ band 3 /band 2 were most useful on quartzitic sandstone and siliceous crystalline substrates, while semi-automated methods (supervised classification) performed best on carbonate derived substrates (Wolken, 2006). All identifiable end moraines and trimlines on Cumberland Peninsula, southern Baffin Island were delineated manually from ASTER images (Svoboda and Paul, 2009)

Outlines of the Devon Island ice cap and glaciers on Bylot Island for the period 1956-1961 were mapped by on-screen digitizing from scanned 1:60,000 aerial photographs that were georeferenced using ground control points derived from the Landsat or ASTER imagery and orthorectified with digital elevation data from the Canadian Digital Elevation Dataset (CDED) using either PCI Orthoengine or ERDAS Imagine software (Burgess and Sharp, 2004; Dowdeswell et al., 2007). CDED data are derived from 1:250,000 topographic map sheets (National Topographic Database; NTDB) which were created from 1956-61 aerial photography, and provide the most comprehensive early topographic dataset for the region. For the QEI (excluding the Devon Island ice cap), digital glacier outlines derived from the 1:250,000 map sheets were used to define the ca. 1960 ice extent (after manual checking against the original aerial photography and correction for gross errors).

For the QEI (excluding Devon Island ice cap) and Bylot Island, the 1999/2000 ice outlines were derived from unsupervised classification of orthorectified Landsat 7 ETM+ images using the normalized-difference snow index (NDSI; Dozier, 1984; Sharp et al., 2003; Dowdeswell et al., 2007). NDSI exploits the difference between the high reflectivity of snow and ice in band 2 and its low reflectivity in the near-infrared band 5 (NDSI = (Band 2 –Band 5)/(Band 2 + Band 5)). A Landsat 5 scene from 1993 was used to map recent ice extent on Melville Island as suitable Landsat 7 images were not available. ASTER imagery from June-August 2000-2002 was used to derive outlines for the ~417 km^2 of glacier ice in the region of the QEI between 82°N and 83°N which lies outside the Landsat 7 mask. All images used were acquired in July/August when off-ice snow cover is minimal, and are mostly cloud-free. After initial classification, manual editing was required to correct for misclassification of shadowed areas and ice-covered water bodies. The outline of Devon Island ice cap (and bedrock regions within the ice cap) was derived by on-screen digitizing of orthorectified ETM+ images (Burgess and Sharp, 2004).

For mapping glaciers on the Cumberland Peninsula, Svoboda and Paul (2009) used a mixture of ASTER images and imagery from the Landsat Thematic Mapper (TM) and MultiSpectral Scanner (MSS) sensors. When mapping with ASTER or TM, they used thresholded band ratios (either red/SWIR or NIR/SWIR) to define ice covered areas, with an additional threshold in the green or blue band to distinguish snow and ice from rock in shadowed areas. With MSS, bands 1-3 were used to map illuminated snow and clean ice. As the MSS sensor has no SWIR band, a NIR band was used to define a band ratio (MSS3/MSS4) with which to map snow and ice in shadowed areas, with an additional

threshold in band 3 to remove wrongly classified rocks in shadow. Manual procedures were used to map debris-covered ice, and to edit out snowfields and turbid water bodies that were misclassified as glaciers.

Results

High resolution stable isotope and melt layer records derived from ice cores from ice caps in the QEI suggest that the Little Ice Age (LIA) in the region began around 1500 AD and lasted until as late as 1925 AD in some regions (Fisher et al., 1983; Koerner and Fisher, 1990; Kinnard et al., 2008). Subsequent warming, which peaked in the late 1950s and early 1960s, resulted in a substantial reduction in terrestrial ice cover in the QEI. This produced extensive areas of poorly vegetated terrain that extend back to modern glacier margins and are delineated by abrupt trimlines or moraines that record the former extent of perennial snow and ice cover (Wolken et al., 2008a; Svoboda and Paul, 2009; Plate 4). Mapping of these shows a 37% (62 387 km^2) decrease in the area of terrestrial ice in the QEI between the end of the LIA and 1960. This was most marked in the eastern QEI, but ice cover was completely removed from many of the western islands by 1960 (Wolken et al., 2008a). On Cumberland Peninsula, southern Baffin Island, glacier area decreased by 7.3% between the end of the LIA and 1975 (Paul and Svoboda, 2009).

Where the trimlines mark the former boundaries of perennial snow patches or near stagnant plateau ice caps (i.e. where the ice mass was not big enough to flow significantly), they also define the former equilibrium-line altitude (ELA) in the region. The increases in equilibrium line altitude (ELA) associated with the pre-1960 ice cover reduction reached 300-600 m in a region that extends from Devon Island into southern Ellesmere and Axel Heiberg Islands, north into the lowlands between Axel Heiberg and Ellesmere Islands, and eventually into the plateaus and mountains of northern Ellesmere Island. Smaller ELA increases (<100 m) occurred in the central and western QEI and western Melville Island, along the coastal fringes of northern Axel Heiberg and northwest Ellesmere Islands, and adjacent to Baffin Bay in the southeastern QEI (Wolken et al., 2008a). This pattern of ELA change is broadly consistent with the primary mode of variability (1st Empirical Orthogonal Function) in summer 2 m air temperature (1949-2002) over the QEI from the NCEP/NCAR Reanalysis, which shows maximum variation over the interior of the QEI. Thus, this same spatial pattern of summer temperature change may have characterized the transition from the Little Ice Age to the warmer conditions of the 20th century in the QEI. Changes in mean summer 2 m air temperature associated with the mapped ELA changes were estimated using a summer near-surface temperature lapse rate of −4.3ºC/km, based on observations on

Prince of Wales Icefield, Ellesmere Island (Marshall *et al.*, 2007). These changes averaged +1.1ºC (SD = 0.4ºC) for the QEI as a whole, and ranged from <0.5ºC in northwest Axel Heiberg and Ellesmere Islands and western Melville Island, to >2.9ºC in some areas of Ellesmere and Devon Islands (Wolken et al., 2008b).

The reduction in glacier ice area on Bylot Island between 1958-61 and 2000-2001 was 253 km^2 (5.1% of the 1958/61 area; Dowdeswell et al., 2007). Among the larger ice caps on Baffin Island, a total of 290 km^2 of ice was lost from the Barnes (- 2%), Penny (- 1.9%), Terra Nivea (- 14%) and Grinnell (- 10.9%) ice caps between 1958/61 and 2000/1 (E. Dowdeswell, pers comm.). The area of small plateau ice caps in interior northern Baffin Island decreased from 150 km^2 in 1958 to only 67 km^2 in 2005 (- 55%) (Anderson et al., 2008), while on the Cumberland Peninsula in southeast Baffin Island, the cumulative area of 264 glaciers decreased by 12.5% between ~1920 and 2000 (Paul and Svoboda, 2009). In the latter study, proportional area reductions were greatest for the smallest glaciers in the sample and there was evidence that the rate of area loss increased by about 55% after 1975.

In the QEI, the glacier covered area decreased by 2844 km^2 (- 2.7%) between 1959/60 and 2000/1, with the greatest reductions in northern Ellesmere Island (927 km^2; - 3.4%), southern Ellesmere Island (636 km^2; - 5.9%) and Devon Island (609 km^2; - 4%) (Table 1). The proportional area reductions were greatest for glaciers < 1km^2 in area (- 38.7% for the QEI as a whole), and least for the 4 ice caps and icefields > 10,000 km^2 (- 1.4% overall) (Table 2). For instance, the area of the 14,400 km^2 Devon Island Ice Cap decreased by 338 +/- 40 km^2 (2.4%) between 1959/60 and 1999/2000 (Burgess and Sharp, 2004). 91 glaciers in the QEI disappeared completely between 1959/60 and 1999/2000. Braun et al. (2004) describe the shrinkage of small ice caps in northern Ellesmere Island.

Region	~1960 area (km^2)	~2000 area (km^2)	Area change (km^2)	Area change (%)
North Ellesmere	27,556	26,629	-927	-3.4
Agassiz	21,645	21,366	-279	-1.3
Axel/Meighen/Melville	12,231	12,017	-214	-1.7
Prince of Wales	19,558	19,378	-180	-0.9
South Ellesmere	10,696	10,060	-636	-5.9
Devon	15,344	14,735	-609	-4.0
Total QEI	**107,071**	**104,186**	**-2844**	**-2.7**
Bylot	5036 (1958-61)	4783 (2001)	-253	-5.0
Barnes Ice Cap	5995 (1958)	5874	-121	-2.0
Penny Ice Cap	6604 (1959)	6478	-126	-1.9
Terra Nivea Ice Cap	197 (1958)	169	-28	-14
Grinnell Ice Cap	135 (1958)	120	-15	-10.9

Table 1. Changes in the area of ice caps and glaciers in the QEI and Bylot Island, and of selected ice caps on Baffin Island over the period 1958/61 to 1999/2001. Years when images were acquired are given in brackets when not exactly coincident with column header. The "~2000" area of ice caps on Melville Island is from 1993 LandSat imagery. "Agassiz" includes the glaciers of the Fosheim Peninsula and Sawtooth Range, western Ellesmere Island. "South Ellesmere" includes Coburg Island and the ice caps on Devon and Ellesmere Islands in and around the Hell's Gate Polynya.

Initial Area (km^2)	**>10,000**	**1,000-10,000**	**100-1,000**	**60-100**	**10-60**	**5-10**	**1-5**	**<1**
N. Ellesmere	-2.0* (1)	-3.8* (3)	-7.1 (9)	-6.7 (6)	-10.3 (30)	-22.2 (36)	-25.6 (170)	-29.2 (218)
Agassiz	-0.8 (1)		-2.3 (3)	-1.3 (4)	-6.0 (28)	-11.3 (26)	-16.6 (91)	-31.6 (143)
Axel Heiberg		-0.9 (2)	-2.8 (3)	-15.6* (2)	-9.8 (22)	-13.1 (12)	-17.1 (68)	-34.8 (56)
Pr. of Wales	-0.7 (1)				-19.3* (4)	-29.0* (1)	-45.7* (20)	-74.2* (13)
S. Ellesmere		-2.6 (2)	-12.7* (6)	-14.8 *(5)	-21.4* (18)	-27.0* (20)	-44.7* (92)	-64.1* (44)
Devon	-2.2* (1)		-20.5* (4)	-34.6* (1)	-31.4* (6)	-52.7* (9)	-67.4* (37)	-69.8* (56)
QEI	**-1.4**	**-2.6**	**-9.3**	**-10.4**	**-12.5**	**-22**	**-30.5**	**-38.7**

Table 2. Mean percentage area change (1959/60–1999/2000) of glaciers and ice caps in different regions of the QEI as a function of initial ice area (km^2) in 1959/60. Regions with greater than average fractional reduction in glacier area in a given area bin are indicated with an asterisk. The number of ice masses of each size range is given in brackets. Blank cells indicate that there are no glaciers in that size range in that region.

Of 125 major outlet glaciers in the QEI that experienced significant changes in terminus area (> 0.5 km^2) between 1959/60 and 2000/1, 91 receded and 34 advanced. Of the 77 outlets that terminated in tidewater, 54 receded and 23 advanced. Thus the proportion of land-terminating outlet glaciers that retreated (77%) is slightly higher than the proportions of all outlet glaciers (73%) and tidewater outlets (70%) that did so. It is noteworthy that the largest tidewater glaciers draining Prince of Wales Icefield (Trinity and Wykeham Glaciers) have retreated rapidly since the early 2000s (Plate 5). The changes in glacier dynamics and ice thickness associated with this retreat are still being investigated.

Key issue

Changes in glacier surface elevation and volume; sea level contributions

Regular measurements of surface mass balance in the Canadian Arctic are restricted to a few generally small glaciers, with the exception of a mass balance transect in the northwest sector of the Devon Island Ice Cap that has been monitored annually since 1961 (Koerner, 2005). The extent to which these measurements can be extrapolated to the entire regional ice cover and, in particular, the larger ice caps is uncertain. As a result, there have been several recent attempts to estimate volume changes of

entire ice caps from repeat measurements of ice cap surface height derived by airborne (Abdalati et al., 2004) or satellite (Gardner et al, 2011) laser altimetry, or stereo photogrammetry (Sneed et al., 2008). An alternative approach is based on repeat satellite gravimetry (GRACE; Gardner et al., 2011). Other estimates of volume change rates have been based upon modeled surface mass balances and/or computed iceberg calving fluxes (Mair et al., 2005, 2009; Hüss et al., 2008; Gardner and Sharp, 2009; Burgess et al., 2005; Shepherd et al., 2007; Gardner et al., 2011), or on the difference between local surface mass balance and local flux divergence (Burgess and Sharp, 2008). Only the work of Gardner et al. (2011) provides a comprehensive assessment of the overall mass balance of the entire Canadian Arctic land ice cover that takes into account all ice masses and mass losses by both melt/runoff and iceberg calving. This assessment covers the period 2004-2009.

Based on repeat airborne laser altimetry surveys over Canadian Arctic ice caps in 1995 and 2000, Abdalati et al. (2004) suggested that the regional mass balance for Arctic Canada for the period 1995-2000 was on the order of -25 km^3 a^{-1} of ice, equivalent to 0.064 mm a^{-1} of sea level rise. These surveys indicated that most ice caps were thinning at elevations below 1600m and thickening or maintaining a constant thickness at higher elevations. Hüss et al. (2008) reported a similar pattern for the Laika Glacier on Coburg Island. Low elevation thinning on the Barnes and Penny Ice Caps exceeded 1 m a^{-1}, while in the QEI it was generally less than 0.5 m a^{-1} (Abdalati et al., 2004). This variation in the rate of low elevation thinning is consistent with regional variations in the rate of glacier area reduction. For the southern Barnes Ice Cap, Sneed et al. (2008) compared elevation measurements made by ground survey (1970-84), ASTER digital elevation models (2006), and IceSat laser altimetry (2004-06), and found an acceleration in thinning rates from 0.12 m a^{-1} for the period 1970-1984, to 0.76 +/- 0.35 m a^{-1} for the period 1984-2006, and 1.0 +/- 0.14 m a^{-1} for the period 2004-2006. This trend is consistent with the trends in summer temperature shown in Figures 2 and 3, suggesting that thinning rates in this region are controlled primarily by climatic, rather than dynamic, processes.

The causes of high elevation thickening are unclear. Data from meteorological stations show recent precipitation increases that might explain it (Abdalati et al., 2004), but data from shallow ice cores and mass balance stakes on the Devon Island Ice Cap both suggest recent reductions in accumulation at high elevations (Colgan et al., 2008). The ice cores also show a recent increase in the ice content of firn, suggesting an increase in the rate of firnification. In the absence of an increase in precipitation, this would result in ice cap thinning, rather than thickening (Colgan et al., 2008). An alternative explanation of the thickening is a recent reduction in the rate of ice outflow from high

elevation regions of ice caps (Koerner, 2005), perhaps due to propagation of the Little Ice Age cooling wave to the base of the ice caps, causing stiffening and slower deformation of ice near the glacier bed (Colgan et al., 2008).

Various attempts have been made to simulate the surface mass balance of large ice caps in Arctic Canada. Mair et al. (2005) computed a 37 year (1963-2000) mean net surface mass balance of the Devon Island Ice Cap using measurements of net accumulation from shallow ice cores to define the net balance in the accumulation area, and a positive degree day model to compute the surface mass balance of the ablation area. This model was driven by air temperatures measured at Resolute Bay, calibrated to on-ice air temperature measurements. The estimated net balance was -1.6 Gt (or - 0.13 m w.e.) a^{-1}. Gardner and Sharp (2009) computed the net surface balance of the same ice cap for 1980-2006 using precipitation fields derived from the North American Regional Reanalysis (NARR; Mesinger et al. 2006) and a positive degree day model driven by NARR 2m air temperatures for the ice cap summit elevation downscaled to the rest of the ice cap using a variable daily lapse rate method. Their estimate of the annual mean net balance was -0.333 ± 0.12 m w.e. a^{-1}, which agrees very well with long term measurements of mass balance made in the northwest of the ice cap. Shepherd et al. (2007) estimated the specific net surface balance for 1996 (a year when measured net balance was relatively positive) to be + 0.028 m w.e. a^{-1} using perturbed historical accumulation measurements and a positive degree day melt model driven by temperature data from the International Arctic Buoy Program extrapolated over the ice cap using a constant lapse rate. The differences between these estimates are partly explained by differences between the summer meteorological conditions in the periods to which the estimates relate, and by differences in the methods used.

Iceberg calving also contributes significantly to mass loss from the Devon Island Ice Cap. Burgess et al. (2005) estimated an annual mean flux for the period 1960-2000 of -0.51 ± 0.12 km^3 ice a^{-1}. If this flux is assumed to be constant over time and is added to the net surface balance estimates of Mair et al. (2005) or Gardner and Sharp (2009), it implies an overall annual specific net balance for the ice cap of either -0.17 m w.e. a^{-1} (1963-2000) or -0.37 m w.e. a^{-1} (1980-2006) respectively. These estimates equate to contributions to eustatic sea level rise of either 0.21 mm (0.006 mm a^{-1}; 1963-2000) or 0.34 mm (0.0133 mm a^{-1}; 1980-2006).

Mair et al. (2009) estimated the net mass balance of the Prince of Wales Icefield (1963-2003) from measurements of surface mass balance (from stakes and shallow ice cores) and estimates of iceberg calving. The estimated net surface mass balance is within error of zero (-0.1 ± 0.4 Gt a^{-1}),

probably because of the high snow accumulation in the southeastern part of the Icefield which lies adjacent to the North Open Water Polynya, a year-round source of moisture. Iceberg calving is a highly significant component of mass loss (-1.9 ± 0.2 Gt a^{-1}), making the overall mass balance of the icefield negative (-2 ± 0.45 Gt a^{-1}). This equates to a mean specific net mass balance of -0.1 m w.e. a^{-1}, and an annual contribution to global eustatic sea level rise of 0.005 mm a^{-1}.

Gardner et al. (2011) used three independent approaches (repeat satellite laser altimetry (ICESat), repeat satellite gravimetry (GRACE) and regional scale mass balance modelling to estimate the net mass balance of all glaciers in the Queen Elizabeth Islands, Bylot, and Baffin Islands during the period 2004-2009 (although the mass balance modelling was applied only to the Queen Elizabeth Islands). The mean rate of mass loss for the whole period was estimated to be -61 ± 7 Gt a^{-1}, equivalent to 0.17 ± 0.02 mm a^{-1} of sea level rise. However, the mean rate of mass loss increased sharply from -31 ± 8 Gt a^{-1} in 2004-2006 (a rate only marginally higher than Abdalati et al's (2004) estimate for 1995-2000) to -92 ± 12 Gt a^{-1} in 2007-2009, presumably a result of the summer warming that has occurred since 2005 (Sharp et al., 2011).

Summary and Conclusions

After a period of extensive deglaciation in the early and middle Holocene, glaciers in the Canadian Arctic grew considerably, reaching their maximum extent in the late 19th or early 20th century. Since then, the ice-covered area has decreased substantially. Before 1960, most of the deglaciation involved the shrinkage and disappearance of small glaciers and ice caps, particularly in the western QEI and interior of Baffin Island. Since then, these small ice masses have continued to shrink, but much of the ice-covered area loss has come from the larger ice caps and ice fields. The area of floating ice shelves in northern Ellesmere Island has decreased by around 90% since the early 20th century, with the most recent phase of disintegration occurring since 2000.

Following a decade of peak warmth in the 1950's, summer temperatures decreased in the 1960's and 1970's, before beginning to rise again in the late 1980's and continuing to rise into the 2000's, when average summer temperatures in many areas have been warmer than those encountered in the 1950's. Measurements of glacier surface mass balance reflect this trend, and show increasingly negative balances since 1987 (and especially since 2005), because annual net balance in the region is most strongly influenced by the summer balance. These changes initially reflected a shift in the summer atmospheric circulation over the Arctic that has resulted in increased incursion of warm air from

continental North America into the Arctic Islands since 1987. Since 2005, however, the summer atmospheric circulation has favored strong northward advection of heat into the Canadian Arctic from the North Atlantic (where sea surface temperatures were unusually warm) via Davis Strait and Baffin Bay. Direct measurements of ice cap elevation change show widespread overall thinning, with most rapid thinning at lower elevations. There is now clear evidence from in situ measurements, satellite laser altimetry, satellite gravimetry, and mass balance modelling that rates of thinning and mass loss have increased substantially since 2005.

Iceberg calving is an important loss term in the overall net balance of a number of the larger ice caps and ice fields, but long-term trends in calving rates are not known. There is substantial seasonal and inter-annual variability in the flow rates of tidewater outlet glaciers, and a number of these glaciers are also known to surge. It is therefore likely that variability in calving fluxes may result in significant inter-annual variability in overall net balance. Whether or how this variability is coupled to variability in climate is unclear. These are topics that can now be investigated given the increasing public accessibility of satellite data from missions such as ASTER and the Landsat program. Significant progress has been made recently in estimating the regional contribution of the Canadian Arctic to eustatic sea level change, but the measurements only cover the period since 1995 (and are most comprehensive for the period since 2004). We are still a long way from having a reliable estimate of the long-term trend and short term variability in rates of mass loss from this region.

References

Abdalati, W., W. Krabill, E. Frederick, S. Manizade, C. Martin, J. Sonntag, R. Swift, R. Thomas, J. Yungel, and R. Koerner, 2004: Elevation changes of ice caps in the Canadian Arctic Archipelago. *Journal of Geophysical Research*, **109,** doi:10.1029/2003JF000045.

Ahlnäs, K., and W. M. Sackinger, 1988: Offshore winds and pack ice movement episodes off Ellesmere Island. *In* Sackinger, W.M. and Jeffries, M.O. eds., *Port and Ocean Engineering under Arctic Conditions*: Fairbanks, Alaska, University of Alaska Fairbanks, Geophysical Institute, **3**, 271-286.

Alt, B. T., 1987: Developing synoptic analogs for extreme mass balance conditions on Queen Elizabeth Island ice caps. *Journal of Climate and Applied Meteorology*, **26,** 1605-1623.

Anderson, R. K., G. H. Miller, J. P. Briner, N. A. Lifton, and S. B. DeVogel, 2008: A millennial perspective on Arctic warming from C-14 in quartz and plants emerging from beneath ice caps. *Geophysical Research Letters*, **35,** L01502, doi:10.1029/2007GL032057.

Andrews, J. T., G. Holdsworth, and J. D. Jacobs, 2002: Glaciers of the Arctic Islands. Glaciers of Baffin Island. USGS Professional Paper 1386-J-1, J162-J198 pp.

Bell, C., D. Mair, D. Burgess, M. Sharp, M. Demuth, F. Cawkwell, R. Bingham and J. Wadham, 2008: Spatial and temporal variability in the snowpack of a High Arctic ice cap: implications for mass-change measurements. *Annals of Glaciology*, **48,** 159-170.

Benson, C. S., 1962: *Stratigraphic studies in the snow and firn of the Greenland ice sheet*. *U.S. Army cold regions research and engineering laboratory (CRREL) research report no. 70*, 120 pp.

Bingham, R. G., P. W. Nienow, and M. J. Sharp, 2003: Intra-annual and intra-seasonal flow dynamics of a High Arctic polythermal valley glacier. *Annals of Glaciology, Vol 37*, **37,** 181-188.

Bingham, R. G., P. W. Nienow, M. J. Sharp, and L. Copland, 2006: Hydrology and dynamics of a polythermal (mostly cold) High Arctic glacier. *Earth Surface Processes and Landforms*, **31,** 1463-1479.

Bingham, R. G., A. L. Hubbard, P. W. Nienow, and M. J. Sharp, 2008: An investigation into the mechanisms controlling seasonal speedup events at a High Arctic glacier. *Journal of Geophysical Research*, **113,** F02006, doi:10.1029/2007JF000832.

Blake, W. J., 1981: Neoglacial fluctuations of glaciers, Southeastern Ellesmere Island, Canadian Arctic Archipelago. *Geografiska Annaler*, **63,** 201-218.

Boon, S., and M. Sharp, 2003: The role of hydrologically-driven ice fracture in drainage system evolution on an Arctic glacier. *Geophysical Research Letters* **30**, 1916, doi:10.1029/2003GL018034.

Braun, C., D. R. Hardy, and R. S. Bradley, 2004: Mass balance and area changes of four High Arctic plateau ice caps, 1959-2002. *Geografiska Annaler*, **86A,** 43-52.

Burgess, D. O. and M. J. Sharp, 2004: Recent changes in areal extent of the Devon Ice Cap, Nunavut, Canada. *Arctic, Antarctic, and Alpine Research*, **36,** 261-271

Burgess, D. and M. J. Sharp, 2008: Recent changes in thickness of the Devon Island ice cap, Canada. *Journal of Geophysical Research*, **113,** B07204, doi:10.1029/2007JB005238.

Burgess, D. O., M. J. Sharp, D. W. F. Mair, J. A. Dowdeswell, and T. J. Benham, 2005: Flow dynamics and iceberg calving rates of Devon Ice Cap, Nunavut, Canada. *Journal of Glaciology*, **51,** 219-230.

Cogley, J. G., W. P. Adams, M. A. Ecclestone, F. Jung-Rothenhäusler, and C. S. L. Ommanney, 1996: Mass balance of White Glacier, Axel Heiberg Island, NWT, Canada, 1960-91. *Journal of Glaciology*, **42,** 548-563.

Colgan, W., J. Davis, and M. Sharp, 2008: Is the high-elevation region of Devon Ice Cap thickening? *Journal of Glaciology*, **54,** 428-436.

Copland, L., M. J. Sharp, and J. A. Dowdeswell, 2003: The distribution and flow characteristics of surge-type glaciers in the Canadian High Arctic. *Annals of Glaciology*, **36,** 73-81.

Copland, L., D. R. Mueller, and L. Weir, 2007: Rapid loss of the Ayles Ice Shelf, Ellesmere Island, Canada. *Geophysical Research Letters*, **34,** L21501, doi:10.1029/2007GL031089.

Cress, P. and R. Wyness, 1961: The Devon Island expedition, observations of glacial movements. *Arctic*, **14,** 257–259.

Dowdeswell, J.A., and T.J. Benham, 2003: A surge of Perseibreen, Svalbard, examined using aerial photography and ASTER high resolution satellite imagery. *Polar Research,* **22**, 373-383.

Dowdeswell, E. K., J. A. Dowdeswell, and F. Cawkwell, 2007: On the glaciers of Bylot Island, Nunavut, Arctic Canada. *Arctic, Antarctic, and Alpine Research*, **39,** 402-411.

Dowdeswell, J. A., T. J. Benham, M. R. Gorman, D. Burgess, and M. J. Sharp, 2004: Form and flow of the Devon Island Ice Cap, Canadian Arctic. *Journal of Geophysical Research*, **109,** F02002, doi:10.1029/2003JF000095.

Dozier, J., 1984: Snow Reflectance from Landsat-4 Thematic Mapper. *IEEE Transactions on Geoscience and Remote Sensing*, **22,** 323-328

England, J., N. Atkinson, J. Bednarski, A. S. Dyke, D. A. Hodgson, and C. O. Cofaigh, 2006: The Innuitian Ice Sheet: configuration, dynamics and chronology. *Quaternary Science Reviews*, **25,** 689-703.

England, J., Lakeman, T. R., Lemmen, D. S., Bednarski, J. M., Stewart, T. G., and Evans, D. J. A. 2008: A millennial-scale record of Arctic Ocean sea ice variability and the demise of the Ellesmere Island ice shelves. *Geophysical Research Letters*, **35**, L19502, doi:10.1029/2008GL034470.

Fisher, D. A., R. M. Koerner, W. S. B. Paterson, W. Dansgaard, N. Gundestrup & N. Reeh. 1983: Effect of wind scouring on climatic records from ice-core oxygen-isotope profiles. *Nature* **301**, 205 - 209

Fisher, D. A., R. M. Koerner, and N. Reeh, 1995: Holocene climatic records from Agassiz Ice Cap, Ellesmere Island, NWT, Canada. *Holocene*, **5,** 19-24.

Fisher, D. A., R. M. Koerner, J. C. Bourgeois, G. Zielinski, C. Wake, C. U. Hammer, H. B. Clausen, N. Gundestrup, S. Johnsen, K. Goto-Azuma, T. Hondoh, E. Blake, and M. Gerasimoff, 1998: Penny ice cap cores, Baffin Island, Canada, and the Wisconsinan Foxe Dome connection: Two states of Hudson Bay ice cover. *Science*, **279,** 692-695.

Fitch, A.J., A. Kadyrov, W. J. Christmas, and J. Kittler. 2002. Orientation Correlation. *British Machine Vision Conference 2002*, 133-142.

Gardner, A. S. and M. Sharp, 2007: Influence of the Arctic Circumpolar Vortex on the mass balance of Canadian High Arctic glaciers. *Journal of Climate* **20,** 4586–4598.

Gardner, A. S. and M. J. Sharp, 2009: Sensitivity of net mass balance estimates to near-surface temperature lapse rates when employing the degree-day method to estimate glacier melt. *Annals of Glaciology*, **50,** 80-86.

Gardner, A. S., M. J. Sharp, R. M. Koerner, C. Labine, S. Boon, S. J. Marshall, D. O. Burgess, and D. Lewis, 2009: Near-surface temperature lapse rates over Arctic glaciers and their implications for temperature downscaling for mass balance modeling. *Journal of Climate* **22**, 4281-4298.

Gardner, A.S., Moholdt, G., Wouters, B., Wolken, G.J., Burgess, D.O., Sharp, M.J., Cogley, J.G., Braun, C., and Labine, C. 2001. Sharply increased mass loss from glaciers and ice caps in the Canadian Arctic Archipelago. *Nature* **473**, 357-360.

Hattersley-Smith, G. 1963: The Ward Hunt Ice Shelf: recent changes in the ice front. *Journal of Glaciology*, 4, 415-424.

Hattersley-Smith, G. 1964: Rapid Advance of Glacier in Northern Ellesmere Island. *Nature* **201**, 176.

Hattersley-Smith, G. 1969: Recent observations on the surging Otto Glacier, Ellesmere Island. *Canadian Journal of Earth Sciences* **6**, 883–889.

Haug, T., A. Kaab, and P. Skvarca, 2010: Monitoring ice shelf velocities from repeat MODIS and Landsat data – a method study on the Larsen C ice shelf, Antarctic Peninsula, and 10 other ice shelves around Antarctica. *The Cryosphere* **4**, 31-75.

Holdsworth, G. 1973: Evidence of a surge on Barnes Ice Cap. *Canadian Journal of Earth Sciences* **10**, 1565-1574

Holdsworth, G. 1977: Surge activity on the Barnes Ice Cap. *Nature* **269**, 588-590.

Hooke, R. L. and H. B. Clausen. 1982: Wisconsin and Holocene variations, Barnes Ice Cap, Canada. *Geological Society of America Bulletin,* **93**, 784-789.

Hüss, M., R. Stockli, G. Kappenberger, and H. Blatter, 2008: Temporal and spatial changes of Laika Glacier, Canadian Arctic, since 1959, inferred from satellite remote sensing and mass-balance modeling. *Journal of Glaciology*, **54,** 857-866.

Iken, A., 1974: Velocity fluctuations of an Arctic valley glacier; a study of the White Glacier, Axel Heiberg Island, Canadian Arctic Archipelago. Axel Heiberg Island Research Reports: Glaciology no 5. Montreal, McGill University, 116p.

Jeffries, M. O., 1987: The growth, structure and disintegration of Arctic ice shelves. *Polar Record* **23**, 631-649.

Jeffries, M. O., 1992: Arctic ice shelves and ice islands: Origin, growth and disintegration, physical characteristics, structural-stratigraphic variability, and dynamics. *Reviews of Geophysics*, **30,** 245–267.

Kinnard, C., R. M. Koerner, C. M. Zdanowicz, D. A. Fisher, J. Zheng, M. J. Sharp, L. Nicholson, and B. Lauriol, 2008: Stratigraphic analysis of an ice core from the Prince of Wales Icefield, Ellesmere Island, Arctic Canada, using digital image analysis: High-resolution density, past summer warmth reconstruction, and melt effect on ice core solid conductivity. *Journal of Geophysical Research*, **113,** D24120, doi:10.1029/2008JD011083.

Knight, J. R., C. K. Folland, and A. A. Scaife, 2006: Climate impacts of the Atlantic Multidecadal Oscillation. *Geophysical Research Letters,* **33**, 17, doi:10.1029/2006GL026242.

Koenig, L. S., K. R. Greenaway, M. Dunbar, and G. Hattersley-Smith. 1952: Arctic ice islands. *Arctic*, **5,** 67-103.

Koerner, R. M., 1977: Devon Island Ice Cap - Core Stratigraphy and Paleoclimate. *Science*, **196,** 15-18.

Koerner, R. M., 2002: Glaciers of the Arctic Islands. Glaciers of the High Arctic Islands USGS Professional Paper 1386-J-1, J111-J146 pp.

Koerner, R. M., 2005: Mass balance of glaciers in the Queen Elizabeth Islands, Nunavut, Canada. *Annals of Glaciology*, **42,** 417-423.

Koerner, R. M. and D. A. Fisher, 1990: A record of Holocene summer climate from a Canadian High-Arctic ice core. *Nature*, **343,** 630-631.

Koerner, R. M. and D. A. Fisher, 2002: Ice-core evidence for widespread Arctic glacier retreat in the Last Interglacial and the early Holocene. *Annals of Glaciology*, **35,** 19-24.

Lesins, G., T. J. Duck, and J. R. Drummond, J.R. 2010. Climate trends at Eureka in the Canadian High Arctic. *Atmosphere-Ocean* **48**, 59-80.

Løken, O.H, 1969: Evidence of surges on the Barnes Ice Cap. *Canadian Journal of Earth Sciences,* **6**, 899-901.

Mair, D., D. Burgess, and M. Sharp, 2005: Thirty-seven year mass balance of Devon Ice Cap, Nunavut, Canada, determined by shallow ice coring and melt modeling. *Journal of Geophysical Research-Earth Surface*, **110,** F01011, doi:10.1029/2003JF000099.

Mair, D., D. Burgess, M. Sharp, J. A. Dowdeswell, T. Benham, S. Marshall, and F. Cawkwell, 2009: Mass balance of the Prince of Wales Icefield, Ellesmere Island, Nunavut, Canada. *Journal of Geophysical Research*, **114**, F02011, doi:10.1029/2008JF001082.

Marshall, S., M. Sharp, D. O. Burgess, and F. Anslow. 2007. Surface temperature lapse rate variability on the Prince of Wales Icefield, Ellesmere Island, Canada: Implications for regional-scale downscaling of temperature. *International Journal of Climatology* **27**, 385-398.

Maxwell, J. B., 1980: *The Climate of the Canadian Arctic Islands and Adjacent Waters* Vol. 1, *Climatological Studies*, Environment Canada, Department of Supply Services, 532 pp.

Meier, M.F., and A. Post. 1969: What are glacier surges? *Canadian Journal of Earth Sciences* **6**, 807–817

Mesinger, F., G. DiMego, E. Kalnay, K. Mitchell, P. C. Shafran, W. Ebisuzaki, D. Jovic, J. Woollen, E. Rogers, E. H. Berbery, M. B. Ek, Y. Fan, R. Grumbine, W. Higgins, H. Li, Y. Lin, G. Manikin, D. Parrish, and W. Shi, 2006: North American regional reanalysis. *Bulletin of the American Meteorological Society*, **87,** 343-360.

Műller, F. 1969: Was the Good Friday Glacier on Axel Heiberg Island surging? *Canadian Journal of Earth Sciences,* **6**, 891–894.

Mueller, D. R., W. F. Vincent, and M. O. Jeffries, 2003: Break-up of the largest Arctic ice shelf and associated loss of an epishelf lake. *Geophysical Research Letters*, **30,** 2031, doi:10.1029/2003 GL017931.

Mueller, D. R., W. F. Vincent, and M. O. Jeffries, 2006: Environmental Gradients, Fragmented Habitats, and Microbiota of a Northern Ice Shelf Cryoecosystem, Ellesmere Island, Canada. *Arctic, Antarctic and Alpine Research* **38**, 593-607.

Mueller, D. R., L. Copland, A. Hamilton, and D. Stern. 2008: Examining Arctic Ice Shelves Prior to the 2008 Breakup. *EOS, Transactions of the American Geophysical Union*, **89**, 502-503.

Paterson, W. S. B., R. M. Koerner, D. Fisher, S. J. Johnsen, H. B. Clausen, W. Dansgaard, P. Bucher, and H. Oeschger, 1977: An Oxygen-Isotope Climatic Record from Devon Island Ice Cap, Arctic Canada. *Nature*, **266,** 508-511.

Paul, F. and F. Svoboda. 2009: A new glacier inventory on southern Baffin Island: II. Data analysis, glacier change and applications. *Annals of Glaciology,* **50**, 22-31.

Scambos, T. A., M. J. Dutkiewicz, J. C. Wilson, and R. A. Bindschadler, 1992: Application of Image Cross-Correlation to the Measurement of Glacier Velocity Using Satellite Image Data. *Remote Sensing of Environment*, **42,** 177-186.

Sharp, M.J., L. Copland, K. Filbert, D. Burgess, and S. Williamson. 2003: Recent changes in the extent and volume of Canadian Arctic glaciers. In *Papers and Recommendations: Snow Watch 2002 Workshop and Assessing Global Glacier Recession, Glaciological Data Report* **GD-32**, Boulder, Colorado, NSIDC/WDC for Glaciology, 70-72.

Sharp, M., Burgess, D.O., Cogley, J.G., Ecclestone, M., Labine, C., and Wolken, G.J. 2011. Extreme melt on Canada's Arctic ice caps in the 21st century. *Geophysical Research Letters* **38**, L11501, doi:10.1029/2011GL047381.

Sharp, M. and Wolken, G. 2011. [Arctic]. Glaciers outside Greenland. [in. State of the Climate in 2010]. *Bulletin of the American Meteorological Society* **92** (6), S155-S156.

Shepherd, A., Z. Du, T. J. Benham, J. A. Dowdeswell, and E. M. Morris, 2007: Mass balance of Devon Ice Cap, Canadian Arctic. *Annals of Glaciology*, **46,** 249-254.

Short, N. H. and A. L. Gray, 2005: Glacier dynamics in the Canadian High Arctic from RADARSAT-1 speckle tracking. *Canadian Journal of Remote Sensing*, **31,** 225-239.

Sneed, W. A., R. L. Hooke, and G. S. Hamilton, 2008: Thinning of the south dome of Barnes Ice Cap, Arctic Canada, over the past two decades. *Geology*, **36,** 71-74.

Sturm, M., 1987: Observations on the Distribution and Characteristics of Potholes on Surging Glaciers, *Journal of Geophysical Research*, **92**(B9), 9015–9022.

Svoboda, F., and Paul, F. 2009. A new glacier inventory on southern Baffin Island, Canada, from ASTER data: 1. Applied methods, challenges and solutions. *Annals of Glaciology,* **50**, 11-21.

Vincent, W. F., L. G. Whyte, C. Lovejoy, C. W. Greer, I. Laurion, C. A. Suttle, J. Corbeil, and D. R. Mueller. 2009. Arctic microbial ecosystems and impacts of extreme warming during the International Polar Year. *Polar Science,* **3**, 171-180.

Wang, L., M. J. Sharp, B. Rivard, S. Marshall, and D. Burgess, 2005: Melt season duration on Canadian Arctic ice caps, 2000-2004. *Geophysical Research Letters*, **32,** doi:10.1029/2005GL023962.

Williamson, S., M. Sharp, J. Dowdeswell, and T. Benham, 2008: Iceberg calving rates from northern Ellesmere Island ice caps, Canadian Arctic, 1999-2003. *Journal of Glaciology*, **54,** 391-400.

Wolken, G.J. 2006: High-resolution multispectral techniques for mapping former Little Ice Age terrestrial ice cover in the Canadian High Arctic. *Remote Sensing of Environment* 101, 104–14.

Wolken, G. J., J. H. England, and A. S. Dyke, 2008: Changes in late-Neoglacial perennial snow/ice extent and equilibrium-line altitudes in the Queen Elizabeth Islands, Arctic Canada. *Holocene*, **18,** 615-627.

Wolken, G. J., M. J. Sharp, and J. H. England, 2008: Changes in late-Neoglacial climate inferred from former equilibrium-line altitudes in the Queen Elizabeth Islands, Arctic Canada. *Holocene*, **18,** 629-641.

Wolken, G. J., M.Sharp and L.Wang, 2009, Snow and ice facies variability and ice layer formation on Canadian Arctic ice caps, 1999–2005. *Journal of Geophysical Research (Earth Surface)*, **114**, F03011, doi:10.1029/2008JF001173.

Zdanowicz, C. M., D. A. Fisher, I. Clark, and D. Lacelle, 2002: An ice-marginal delta O-18 record from Barnes Ice Cap, Baffin Island, Canada. *Annals of Glaciology,* **35,** 145-149.

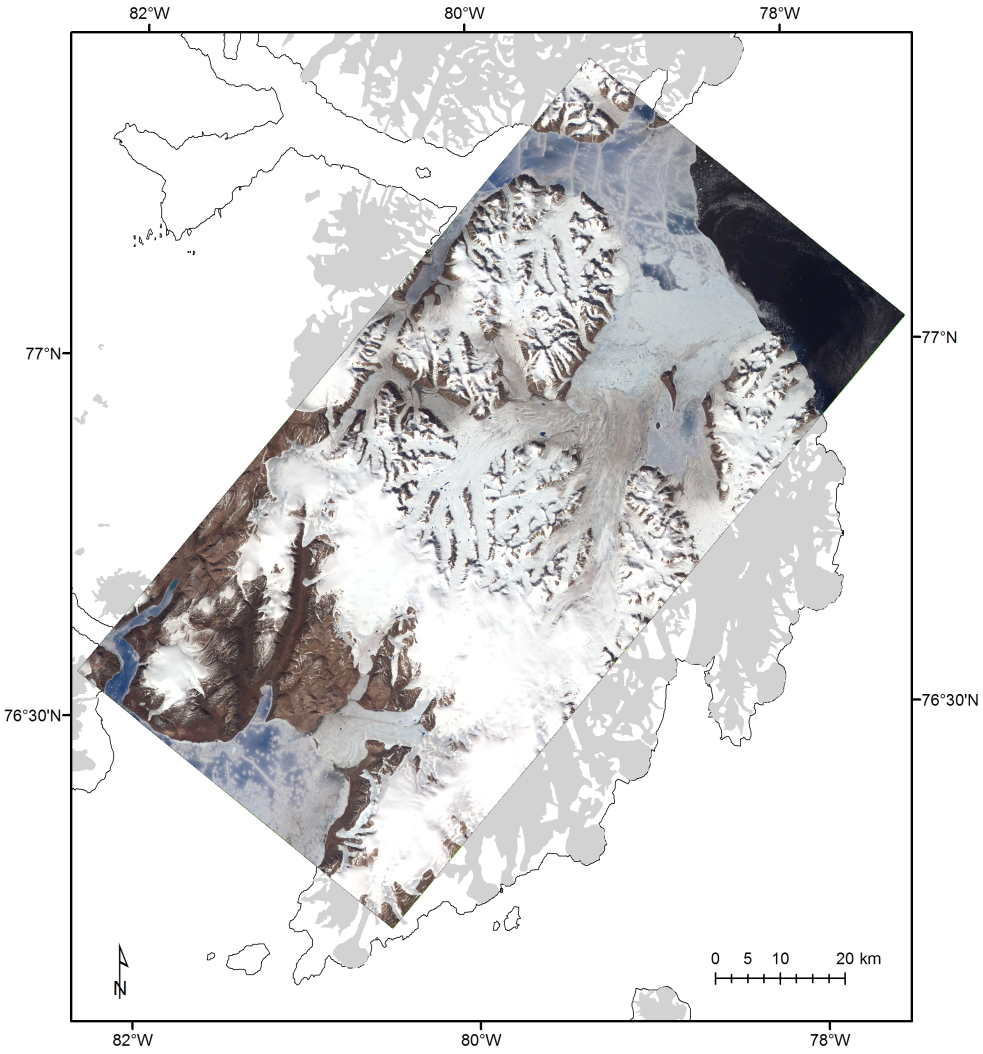

Plate 1: ASTER mosaic of the Manson Icefield, Ellesmere Island. The mosaic was created from two ASTER images (182851 and 182900) acquired on July 3, 2002. Mittie Glacier, flowing northwards into the ocean is actively surging.

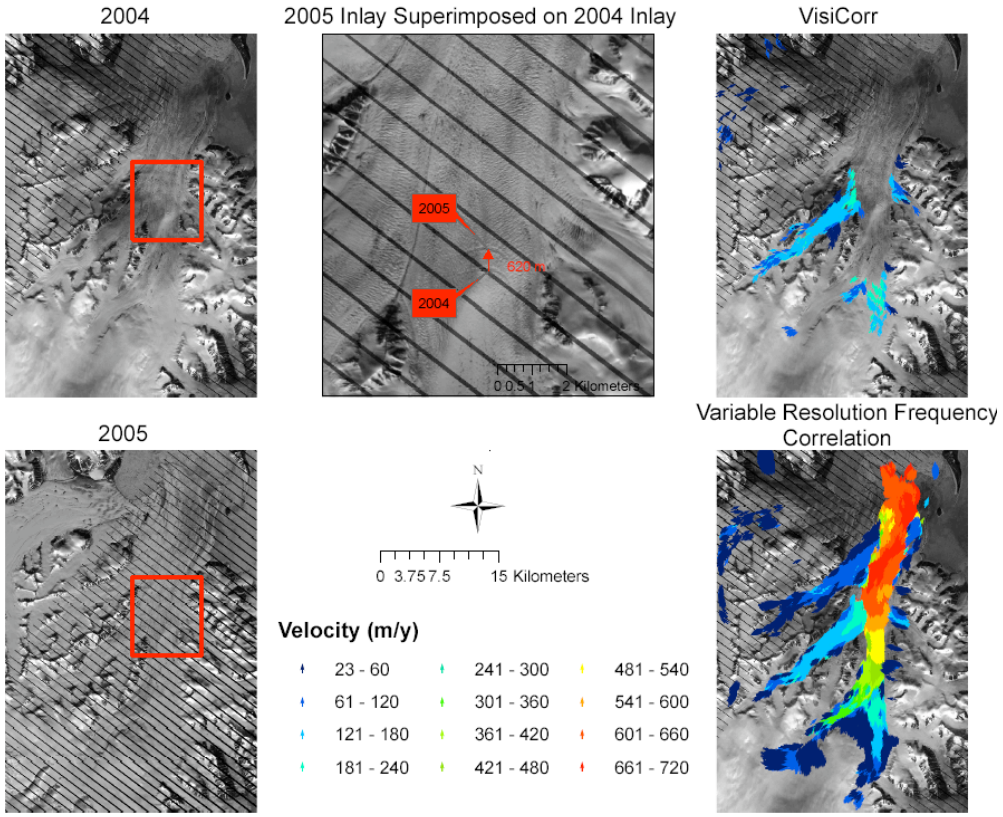

Plate 2. Annual velocity fields for the actively surging Mittie Glacier, Manson Icefield, Ellesmere Island for the year 2004-2005 derived from Landsat 7 ETM+ imagery. The left hand column shows the 2 images used to derive the velocity fields, illustrating image striping in both images (Top: July 10, 2004, Path 038 Row 005. Bottom: July 4, 2005, Path 039, Row 005). The centre figure shows the displacement of a single large crevasse by 620m between the acquisition dates of the 2 images. The right hand column shows velocity fields derived using standard image intensity domain cross correlation methods using the VisiCorr software (top) and an automated variable correlation block size algorithm implemented in the frequency domain (bottom). The frequency domain approach is able to resolve the velocity field over almost the entire glacier, while the standard fixed correlation block size approach (using default search and reference chip values) is only able to resolve velocities on a few of the tributaries. Note: misaligned velocity vector results from both methods, due to correlation blunders, were removed manually.

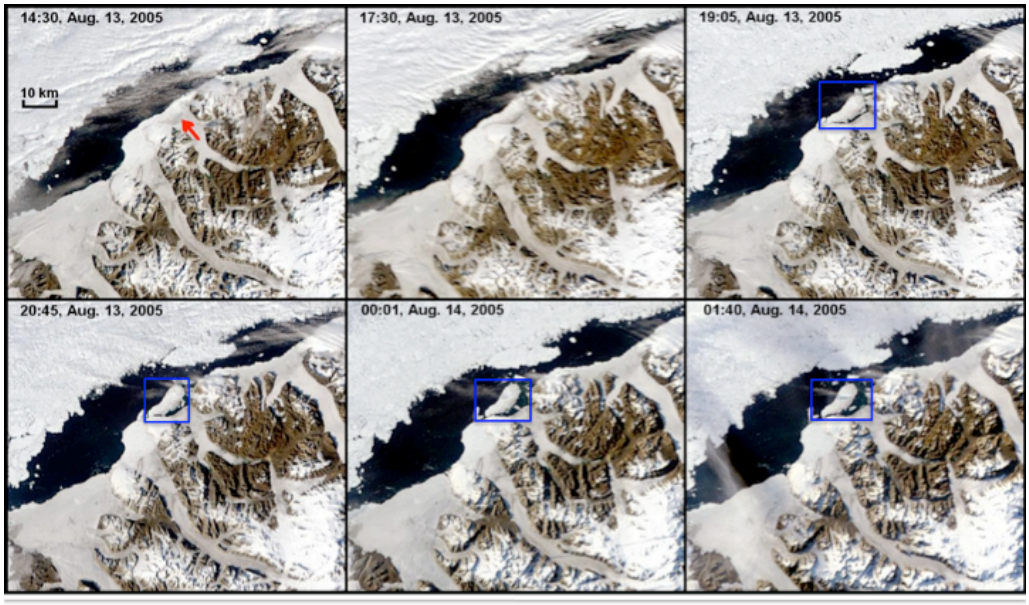

Plate 3: Sequence of MODIS (TERRA & AQUA) satellite images showing the calving of the Ayles Ice Shelf, August 13-14, 2005 (ground resolution ~250 m). Red arrow marks rear of Ayles Ice Shelf prior to separation, while the blue boxes highlight the location of the calved iceberg. All times are in UTC. MODIS data courtesy of MODIS Rapid Response Project (NASA/GSFC and University of

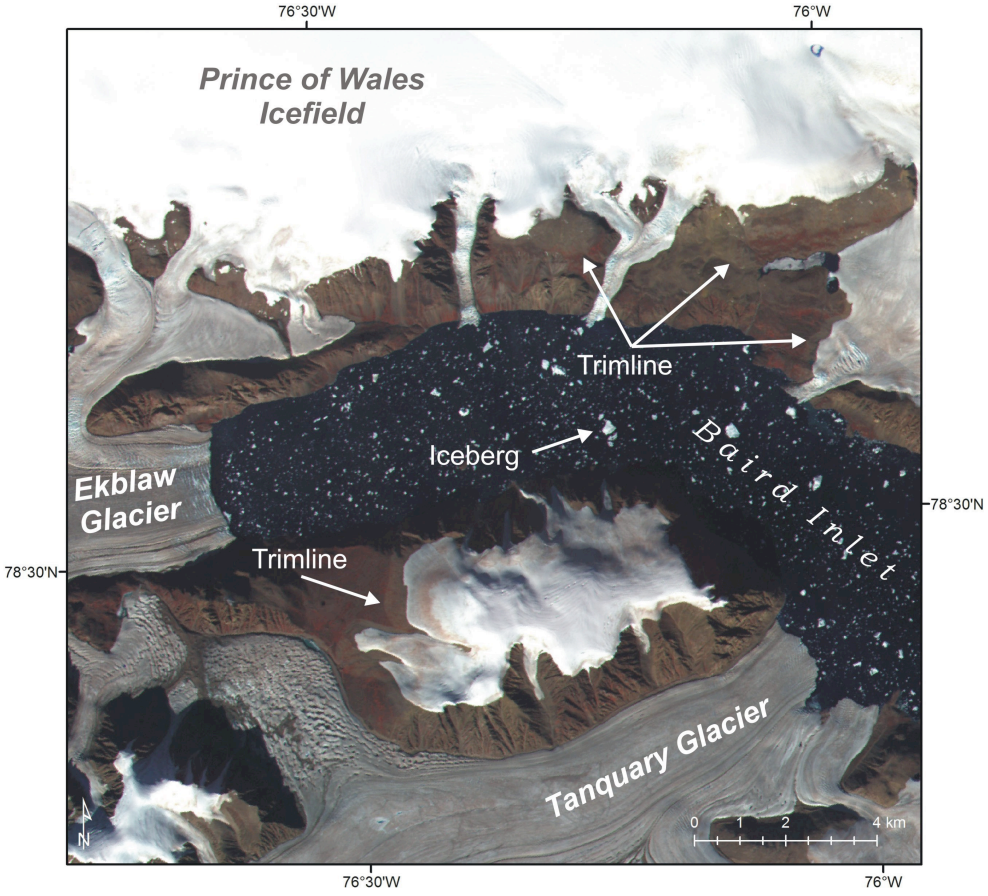

Plate 4: ASTER image (183511), acquired on August 7, 2000, of Ekblaw Glacier, a tidewater outlet glacier that drains eastwards from the Prince of Wales Icefield, Ellesmere Island, into Baird Inlet. The inlet contains numerous large icebergs calved from the surrounding tidewater glaciers. Also visible in this scene are prominent trimlines that define the late 19th and early 20th century limits of many of the glaciers.

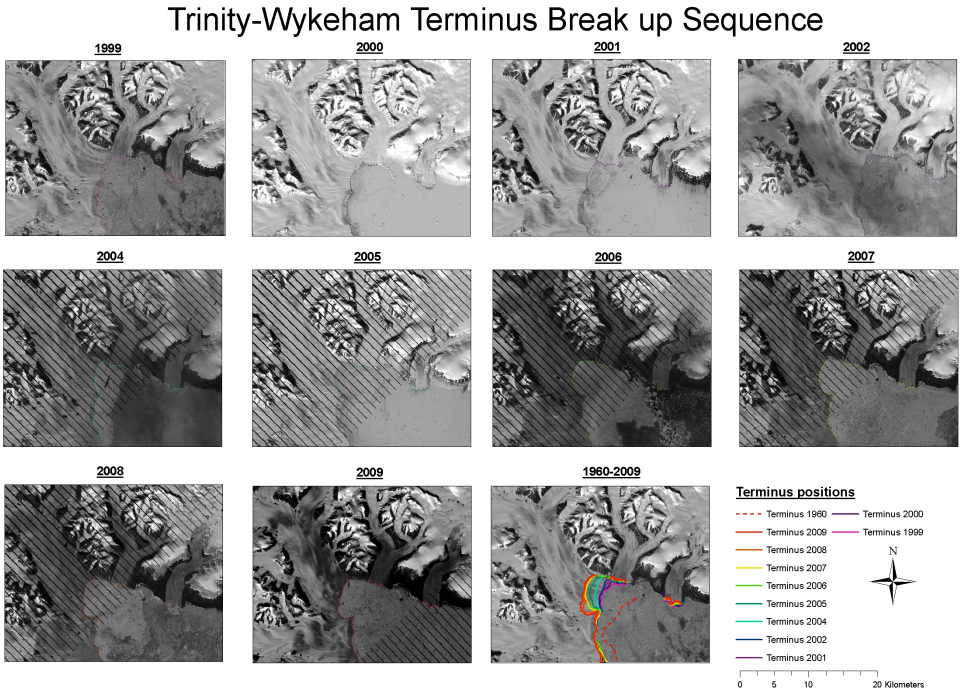

Plate 5: Sequence of Landsat 7 ETM+ panchromatic images showing the recent retreat of the termini of the Trinity and Wykeham Glaciers, eastern Prince of Wales Icefield, Ellesmere Island. These are the 2 largest tidewater glaciers draining the icefield and the major iceberg calving source. Note the acceleration of frontal retreat of Trinity Glacier (the northern part of the joint terminus) after 2002.